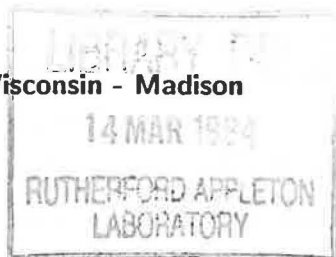




University of Wisconsin - Madison



MAD/PH/807

UCD-93-38

RAL-93-101

December 1993

SINGLE-LEPTON TOP SIGNALS WITH A b -TAG
AT THE TEVATRON

V. Bargér^a, E. Mirkes^a, J. Ohnemus^b, and R.J.N. Phillips^c

^aPhysics Department, University of Wisconsin, Madison WI 53706, USA

^bPhysics Department, University of California, Davis, CA 95616, USA

^cRutherford Appleton Laboratory, Chilton, Didcot, OX11 0QX, UK

HEP

Events with a leptonic W -decay plus jets should contain top-quark signals, but a QCD $W + \text{jets}$ background must be separated. We compare transverse W -momentum, jet multiplicity, and b -tagging separation criteria, and find that the main background after tagging comes from mistagging. We illustrate how to extract the mass m_t via event reconstructions and how to confirm signal purity by lepton angular distributions.

COPY 1 R61 RR
ACCN: 222627

Searches for the t -quark are intense at the Fermilab Tevatron pp collider. The main characteristics of $t\bar{t}$ pair production and decay are well known. Current lower limits on m_t [1] are well above $M_W + m_b$, assuming the Standard Model (SM), so all signals contain $t\bar{t} \rightarrow W^+bW^-\bar{b}$. As an experimental trigger, at least one W is usually required to decay leptonically $W \rightarrow \ell\nu$ ($\ell = e, \mu$), providing a distinctive isolated high- p_T lepton and large missing- p_T (denoted \cancel{p}_T); but large backgrounds, especially from QCD production of $W + \text{jets}$, remain to be separated. If the second W also decays leptonically and one b -jet is tagged, the resulting $\ell\ell'b$ signal may be comparatively clean, but the event rate is not large and the top mass cannot be directly reconstructed due to missing neutrinos [2,3].

The advantages of single-lepton top signals, where the second W decays hadronically $W \rightarrow q\bar{q}$, are both larger event rate and direct top mass reconstructibility; the draw-back here is the inherent uncertainty in QCD $W + \text{jets}$ background calculations at the parton level, especially for high jet multiplicity n_j . Some way must therefore be found to control or eliminate this background. Since the top signals contain four hard partons $b\bar{b}q\bar{q}$ while the QCD background has typically low n_j and few b -quarks, the usual approach is to require large n_j and b -tagging of at least one jet; calculations then predict that the background is severely reduced relative to the signal [4], assuming this background comes mainly from $Wb\bar{b} + \text{jets}$ production with genuine b -jets.

In the present Letter we point out that the main background actually comes from mistagged events containing no true b -jets. We find that the transverse momentum $p_T(W)$ of the trigger W is another important characteristic, and investigate the interplay of $p_T(W)$, n_j , and b -tagging criteria in separating single-lepton top signals from $W + \text{jets}$ backgrounds. The decay $t \rightarrow bW$ has a Jacobian peak at $p_T(W) = (m_t^2 - M_W^2)/(2m_t)$ in the t -restframe, giving a broad $p_T(W)$ lab-frame distribution unlike the QCD background. We find that the background $p_T(W)$ -dependence differs less from the signal after imposing $n_j \geq 3$; nevertheless a $p_T(W)$ cut can be helpful for heavier top $m_t \gtrsim 170$ GeV. Once selection cuts have been imposed, we illustrate how the mass m_t can be found by event reconstructions, with fitting criteria that further suppress backgrounds, and show how the signal purity can eventually

be confirmed by lepton decay distributions. Our conclusions are detailed in (i)–(viii) below.

Analytic next-to-leading order calculations [5] of inclusive W production agree well with CDF data [6] but cannot address jet multiplicity with specific acceptance cuts, and anyway exist only for $n_j \leq 2$. We therefore make Monte Carlo parton-level calculations of $W + n$ -jet backgrounds at leading order [4,7,8], interpreting final partons as jets if they satisfy the cuts, and imposing typical acceptance cuts:

$$p_T(\ell, \text{jet}, \text{missing}) > 20 \text{ GeV}, \quad |\eta(\ell)| < 1.1, \quad |\eta(j)| < 2.0, \quad \Delta R(jj, j\ell) > 0.4. \quad (1)$$

Here $\eta = \ln \tan(\theta/2)$ is pseudo-rapidity, $(\Delta R)^2 = (\Delta\phi)^2 + (\Delta\eta)^2$, and θ and ϕ are polar and azimuthal angles relative to the beam. The ΔR cuts approximate some effects of jet-finding and lepton-isolation criteria. We assume that at least one of the final jets is b -tagged by a vertex detector (neglecting additional tagging via semileptonic decays, since the extra neutrino would blur reconstructions of $t \rightarrow Wb$ kinematics). For $W + \text{jets}$ production, we neglect quark masses (valid at high p_T) and use the scale $Q = \langle p_T(j) \rangle$ with the MRS set D0 parton distributions [9] and 4 flavors. The signals from $t\bar{t}$ production and decay are calculated at lowest order, without t -fragmentation effects because of the short top lifetime. However, we normalize the cross section to $O(\alpha_s^3)$ calculations, taking central values from Ref. [10] (similar central values are given in Ref. [11]). To all calculations we add gaussian lepton- and jet-smearing prescriptions [12], based on CDF values [13], and evaluate p_T from the overall p_T imbalance.

In the CDF experiment, the efficiency for tagging one or more b -jets in a $t\bar{t}$ event is about 0.30, corresponding to a probability $\epsilon_b \simeq 0.16$ per b -jet; the probability of a fake b -tag is estimated to be $\epsilon_q \simeq \epsilon_g \simeq 0.01$ per light-quark or gluon jet [14]. We assume a probability $\epsilon_c \simeq 0.03$ for a bogus c -jet tag. The cross section for each final configuration is multiplied by the corresponding probability that at least one of the jets is tagged; e.g. the tagged cross sections for $Wg g g g$, $Wc\bar{c}g g$, $Wb\bar{b}q q'$ production contain factors 0.04, 0.08, 0.32, respectively.

Tagged signal and background cross sections, for separate jet multiplicities n_j , are shown versus $p_T(W)$ in Fig. 1(a). Solid curves denote the $n_j = 3$ and $n_j = 4$ signals for the case

$m_t = 150 \text{ GeV}$ ($n_j \leq 2$ signals are negligible). Dashed curves show total $n_j = 1, 2, 3, 4$ backgrounds from $W + \text{jets}$. For comparison, the contribution from $Wb\bar{b}j j$ final states, containing two true b -jets [4,8], is shown by a dash-dotted curve. Figure 1(a) shows that

- (i) The backgrounds from $Wb\bar{b} + \text{jets}$ channels that contain genuine b -jets and have attracted most attention [4,8], contribute much less than fake-tags. If cleaner tagging becomes possible, better background suppression will follow.
- (ii) The $W + \text{jets}$ background has narrower $p_T(W)$ dependence than the $t\bar{t}$ signal; the signal gets broader as m_t increases.
- (iii) Higher-multiplicity background components differ less sharply from the signal in their $p_T(W)$ dependence.

Figure 1(b) compares integrated cross sections above a minimum cutoff $p_T(W) > p_T^{\text{min}}$, for multiplicities $n_j = 3, 4$. Dashed curves again denote background, solid (dotted) curves denote signals for $m_t = 150$ (170) GeV; in each case the lower curve refers to $n_j = 4$ and the upper curve refers to the combined $n_j = 3, 4$ cross section. These results point to further conclusions:

- (iv) For any given p_T^{min} and luminosity, $n_j = 4$ is always the best choice. Adding $n_j = 3$ to $n_j = 4$ data gives more signal events S but much more background B , such that both S/B and the statistical significance S/\sqrt{B} are decreased.
- (v) For $m_t \lesssim 150 \text{ GeV}$ with $n_j = 4$, p_T^{min} cuts confer little advantage; they improve S/B but reduce S/\sqrt{B} , leaving cleaner but less significant signals.
- (vi) For heavier top, the broader signal can justify a p_T^{min} cut; e.g. for $m_t = 170 \text{ GeV}$ and $n_j = 4$, a cut $p_T(W) > 50 \text{ GeV}$ increases S/B by 25% with no loss of significance. Greater advantages accrue for yet larger m_t .

With a selected class of 4 jet events with a single-lepton and a b -tag, which are dominantly from $t\bar{t}$, there are various ways to extract m_t (see e.g. Ref. [2,4]); we illustrate three.

- (a) We can infer the neutrino longitudinal momentum from the $W \rightarrow \ell\nu$ mass shell constraint, within a two-fold ambiguity, assuming $\mathbf{p}_T(\nu) = \mathbf{p}_T$. Then the distribution of invariant mass $m(\ell\nu_{b\text{-tag}})$ has a peak at m_t on a combinatorial background. Each of the two

W -solutions is counted independently; also, for multi-tagged events each tagged jet contributes independently to this distribution. It is illustrated in Fig. 2(a) for $m_t = 150$ GeV and $n_j = 4$.

(b) Another approach is to identify two final untagged jets arising from $W \rightarrow jj$, satisfying an approximate mass-shell constraint

$$|m(jj) - M_W| < 15 \text{ GeV}. \quad (2)$$

Then the tagged jet b_1 and the remaining fourth jet b_2 are both presumably b -jets (in the desired $t\bar{t}$ events), and the distributions of invariant mass $m(jj b_1)$ and $m(jj b_2)$ each contain a peak at m_t on a combinatorial background (that is smaller because no two-fold ambiguity is present in $W \rightarrow jj$). This approach is illustrated in Fig. 2(b), for $m_t = 150$ GeV and $n_j = 4$; the distributions $m(jj b_1)$ and $m(jj b_2)$ are summed, giving 2 counts per event. It makes no difference here whether one or both of the non- W jets are tagged; both are regarded as b -jets.

(c) A better method is to reconstruct both leptonic and hadronic W 's. There are then 4 ways to pair these W 's (one W still has the two-fold ambiguity) with the two remaining jets (presumed to be b and \bar{b}); each pairing gives two top masses m_{t1} and m_{t2} . We select the pairing in which m_{t1} and m_{t2} are closest, subject to a reasonable limit

$$|m_{t1} - m_{t2}| < 50 \text{ GeV}, \quad (3)$$

and their mean value defines the reconstructed top mass \tilde{m}_t :

$$\tilde{m}_t = (m_{t1} + m_{t2})/2. \quad (4)$$

The two-fold $W \rightarrow \ell\nu$ ambiguity and pairing ambiguities are thus resolved [12] and a sharper t -mass peak results, as shown in Fig. 2(c) for $m_t = 150$ GeV with $n_j = 4$. The integrated $t\bar{t}$ signal here is 0.22 pb and the background is 0.017 pb, corresponding to 4.6 events on a background of 0.4 events with the present accumulated luminosity 21 pb^{-1} at CDF. For $m_t = 170$ GeV the signal is 0.12 pb. Figure 2 indicates a further conclusion:

(vii) Full reconstruction as in (c) gives the cleanest and narrowest peak, hence best m_t resolution.

We note that a different kind of approach is to use a maximum-likelihood analysis on individual signal events [15], with the background suppressed by tagging with $p_T(W)$ and/or n_j cuts.

The final event sample, after all cuts, can be examined to confirm the characteristics expected of a $t\bar{t}$ signal. First, the $p_T(W)$ distribution should agree with Fig. 1. Second, the charged-lepton rapidity distribution should be forward/backward symmetric, unlike QCD W -events; Fig. 3(a) compares the asymmetry $A(y_\ell) = \pm[d\sigma/dy(y_\ell) - d\sigma/dy(-y_\ell)]/[d\sigma/dy(y_\ell) + d\sigma/dy(-y_\ell)]$ for charged leptons. (The \pm sign is equal to the lepton's charge and $y > 0$ is the hemisphere in the p beam direction.) Also decay distributions in the Collins-Soper frame [16] (where the $W \rightarrow \ell\nu$ reconstruction gives simply a $\pm \cos\theta$ ambiguity), offer further distinctive differences between signal and background [17]; see Figs. 3(b) and 3(c). There are shape differences in both ϕ and $|\cos\theta|$ distributions, especially the latter. We conclude

(viii) Charged lepton distributions offer additional purity checks on a selected $t\bar{t}$ signal.

ACKNOWLEDGMENTS

VB and RJNP thank Peter Landshoff and John Taylor for the hospitality of DAMTP, Cambridge, where some of this work was done. This research was supported in part by the U.S. Department of Energy under Contracts No. DE-AC02-76ER00881 and No. DE-FG03-91ER40674, in part by the Texas National Research Laboratory Commission under Grants No. RGFY93-221 and No. RGFY93-330, and in part by the University of Wisconsin Research Committee with funds granted by the Wisconsin Alumni Research Foundation.

REFERENCES

- [1] CDF Collaboration: Cornell conference report; D0 Collaboration: Cornell conference report.
- [2] H. Baer et al., Phys. Rev. **D42**, 54 (1990).
- [3] T. Han and S. Parke, Phys. Rev. Lett. **71**, 1494 (1993).
- [4] F. A. Berends, H. Kuijf, B. Tausk, and W. T. Giele, Nucl. Phys. **B357**, 32 (1991); F. A. Berends, J. B. Tausk, and W. T. Giele, Phys. Rev. **D47**, 2746 (1993).
- [5] P. B. Arnold and M. H. Reno, Nucl. Phys. **B319**, 37 (1989); **B330**, 284 (E) (1990); P. B. Arnold and R. P. Kauffman, Phys. Lett. **B349**, 381 (1991); R. J. Gonsalves et al, Phys. Rev. **D40**, 2245 (1989).
- [6] CDF collaboration: F. Abe et al., Phys. Rev. Lett. **66**, 2951 (1991).
- [7] V. Barger et al., Phys. Rev. Lett. **62**, 1971 (1989); Phys. Rev. **D40**, 2888 (1989).
- [8] M. L. Mangano, Nucl. Phys. **B405**, 536 (1993); Z. Kunszt, Nucl. Phys. **B247**, 339 (1984).
- [9] A. D. Martin, R. G. Roberts, and W. J. Stirling, Phys. Rev. **D47**, 867 (1993).
- [10] E. Laenen, J. Smith, and W. L. van Neerven, FERMILAB-Pub-93/270-T.
- [11] R. K. Ellis, Phys. Lett. **B259**, 492 (1991).
- [12] V. Barger, J. Ohnemus, and R. J. N. Phillips, Phys. Rev. **D48**, 3953 (1993).
- [13] CDF collaboration: F. Abe et al, Phys. Rev. **D45**, 3921 (1992).
- [14] See for example H. Frisch, talk at the *XXIII International Symposium on Multiparticle Physics*, Aspen, Colorado, September 1993.
- [15] K. Kondo, J. Phys. Soc. Jpn. **57**, 12 (1988); G. R. Goldstein, K. Sliwa, and R. H. Dalitz, Phys. Rev. **D47**, 967 (1993).
- [16] J. C. Collins and D. E. Soper, Phys. Rev. **D16**, 2219 (1977).
- [17] E. Mirkes, Nucl. Phys. **B387**, 3 (1992).

FIGURE CAPTIONS

- Fig. 1. $p_T(W)$ and n_j characteristics of b -tagged $t\bar{t}$ signals (solid and dotted curves), total $W + \text{jets}$ backgrounds (dashed curves), and the background contribution from $Wb\bar{b}jj$ events (dash-dotted curve): (a) differential cross sections versus $p_T(W)$ for various jet multiplicities n_j , (b) integrated cross sections for $p_T(W) > p_T^{\min}$.
- Fig. 2. Illustrations of three invariant mass reconstructions described in the text, for the case $m_t = 150$ GeV with $n_j = 4$: (a) leptonic $W + b$, (b) hadronic $W + b$, (c) best fit to $t\bar{t}$ kinematics.
- Fig. 3. Angular distributions of charged leptons, after cuts: (a) forward/backward asymmetry versus lepton rapidity y_ℓ , (b) Collins-Soper azimuthal dependence, (c) Collins-Soper $|\cos\theta|$ dependence. Solid (dashed) curves denote $t\bar{t}$ signals ($W + \text{jets}$ backgrounds).

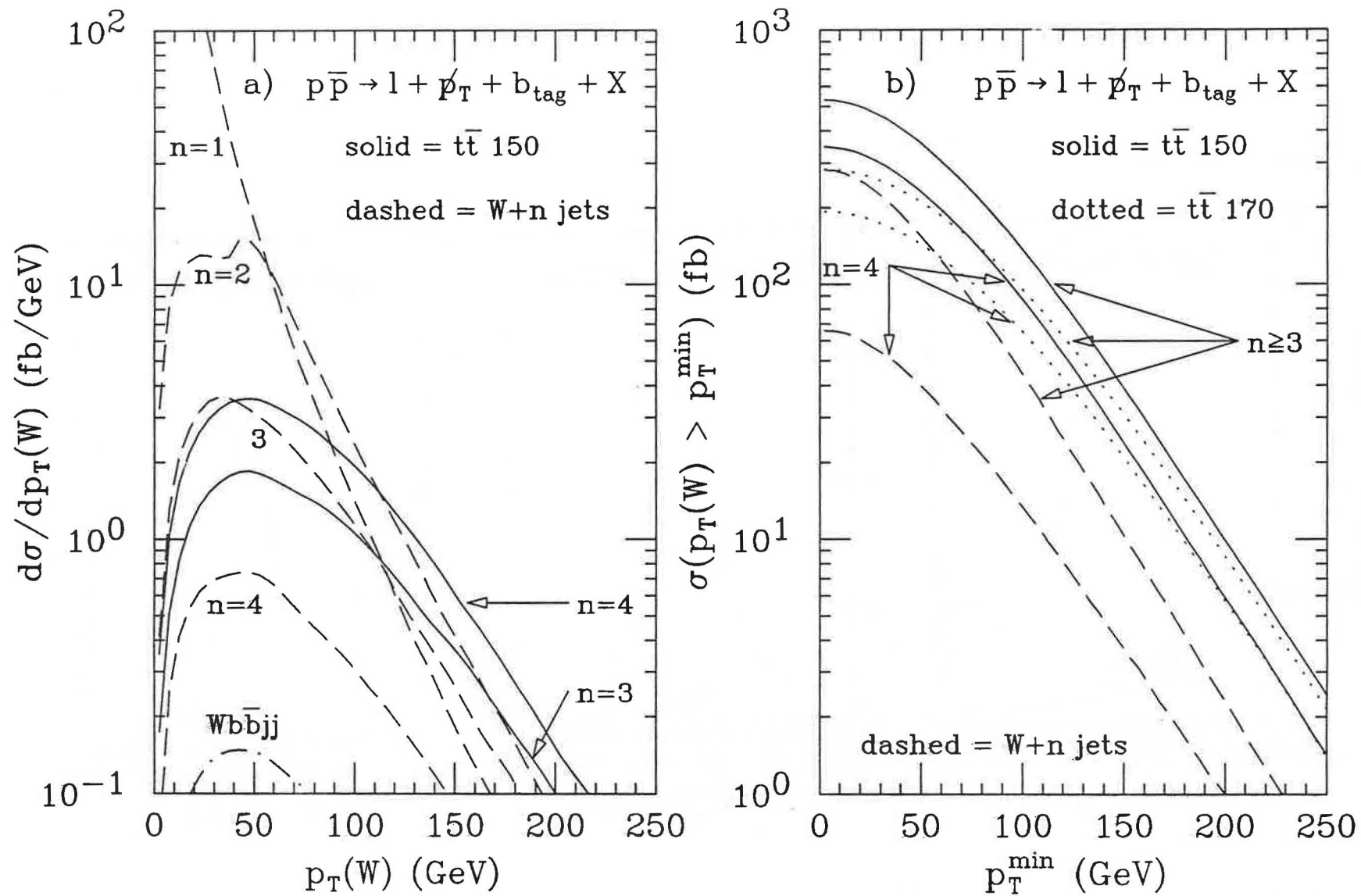


Figure 1

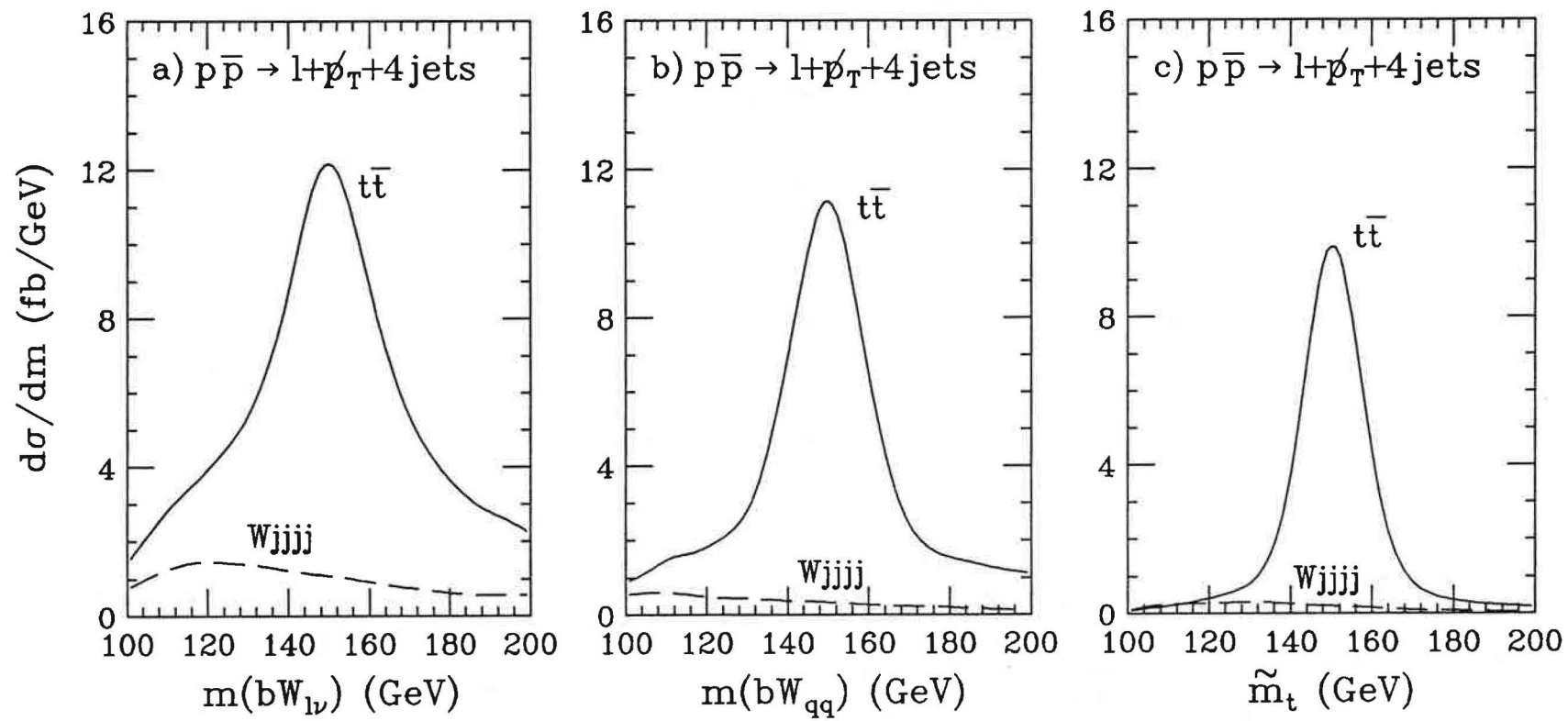


Figure 2

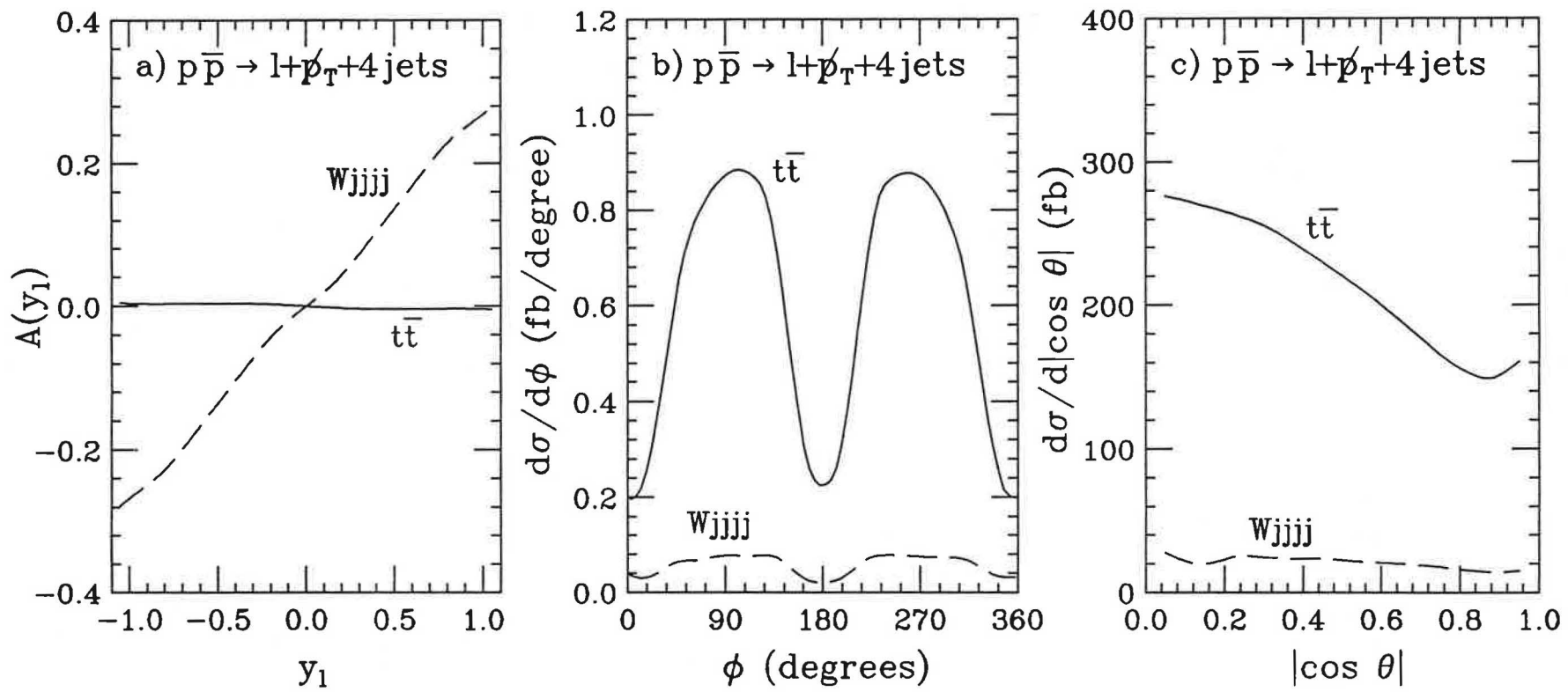


Figure 3

